

Influence of Satellite'S Elevation on the Detection of Triple-Frequency Cycle Slip for GPS

Xiangxiang Fan^a, Xurong Dong^b, and Weiyi Shuai^{c,*}

Space Engineering University, Beijing, China

^axiangx_fan@163.com, ^brongerdx@163.com, ^cshuaiweiyiswy@126.com

*Corresponding author

Keywords: GPS, triple-frequency, cycle slip, elevation, code-phase combination

Abstract: The detection and repair of cycle slip are very important for high-precision positioning. Detection cycle slip for triple-frequency detect method should be as small as possible and elevation of satellite become a factor that cannot be ignored. First, three optimal linear independent combinations for GPS are selected to detect cycle slip. Then the equation of success rate of cycle slip detection and elevation is derived, 40 degree is set as threshold for cycle slip detection. When elevation is higher 40 degree, overall detection success rate is above 96.91%. Finally, data of GPS is tested to observe the actual detection of the cycle slip. The result shows that WL and NL combinations are affected by elevation and have obvious changes. Due to code observation in EWL combination, elevation has a smaller impact on EWL combination.

1. Introduction

The detection and repair of cycle slip are a prerequisite for high-precision positioning. A cycle slip is a discontinuity of an integer number of cycles in the carrier phase observations.

In the triple-frequency cycle slip detection, elevation of satellite becomes a factor that cannot be ignored, especially on the detection of small cycle slips. The most popular method for triple-frequency cycle slip is based on the combinations of code and carrier phase. Zhao [1] used first-order time-difference extra-wide lane (EWL), wide lane (WL) and narrow lane (NL) combinations to form linearly independent combination. Huang [2] used two GF phase combinations and one GF code-phase linear combination to detect cycle slip, which based on LAMBDA and principle of minimum least squares. These methods assume that the ionospheric delay varies smoothly over time. The effect of these methods may be reduced under high ionospheric activity. Yao [3] and Li [4] further proposed to compensate for ionospheric bias by using ionospheric prediction.

Many methods are dedicated to eliminating the effects of the ionosphere in cycle slip detection. To improve success ratio of detection, we must take elevation of satellite into consideration. When elevation of satellite is too low, the received signal usually has a lot of noise, which will seriously affect the detection of cycle slips, especially in insensitive cycle slips.

2. Pseudorange and carrier phase equations

The undifferenced pseudorange and carrier phase equations can be expressed as:

$$P_i = \rho + q_i I + \varepsilon_{P_i} \quad (1)$$

$$\lambda_i \varphi_i = \rho - q_i I + \lambda_i N_i + \varepsilon_{\varphi_i} \quad (2)$$

Where the index i ($i=1,2,3$) refers to a specific frequency of GPS. P and $\lambda\varphi$ are pseudorange and carrier phase measurements in meters, respectively. φ is carrier phase measurement in cycles. ρ is the geometric parameter between the receiver and satellite, the symbol

I denotes the ionospheric delay on frequency f_i in meters, and $q_i = f_1^2 / f_i^2$ is the ionospheric scale factor (ISF) which means the amplification factor for different frequencies. λ_i is the wavelength of frequency f_i , N_i is the integer ambiguity of f_i . ε_{p_i} contains code measurement and multipath noise and ε_{φ_i} is the carrier phase observation noise measured in the meter.

$f_1 = 1575.42 \text{ MHz}$, $f_2 = 1227.60 \text{ MHz}$, $f_3 = 1176.45 \text{ MHz}$.

The combination of code and phase can be expressed [5]:

$$\begin{aligned} P_{(l,m,n)} &= lP_1 + mP_2 + nP_3 \\ &= \rho + \beta_{(l,m,n)}I + \varepsilon_{p_{(l,m,n)}} \end{aligned} \quad (3)$$

$$\begin{aligned} \lambda_{(i,j,k)}\varphi_{(i,j,k)} &= \frac{if_1\lambda_1\varphi_1 + jf_2\lambda_2\varphi_2 + kf_3\lambda_3\varphi_3}{if_1 + jf_2 + kf_3} \\ &= \rho - \beta_{(i,j,k)}I + \lambda_{(i,j,k)}N_{(i,j,k)} + \varepsilon_{\varphi_{(i,j,k)}} \end{aligned} \quad (4)$$

$\beta_{(l,m,n)}$, $\beta_{(i,j,k)}$, $\lambda_{(i,j,k)}$ and $N_{(i,j,k)}$ can be derived as:

$$\beta_{(l,m,n)} = l + m \frac{f_1^2}{f_2^2} + n \frac{f_1^2}{f_3^2} \quad (5)$$

$$\beta_{(i,j,k)} = \frac{f_1^2(i/f_1 + j/f_2 + k/f_3)}{if_1 + jf_2 + kf_3} \quad (6)$$

$$\lambda_{(i,j,k)} = \frac{c}{if_1 + jf_2 + kf_3} \quad (7)$$

$$N_{(i,j,k)} = iN_1 + jN_2 + kN_3 \quad (8)$$

Where the combination coefficients l, m, n should meet the equation $l + m + n = 1$.

$\mu_{(i,j,k)}$ is the phase noise factor and it can be derived as:

$$\mu_{(i,j,k)}^2 = \frac{(if_1)^2 + (jf_2)^2 + (kf_3)^2}{(if_1 + jf_2 + kf_3)^2} \quad (9)$$

Hence the variances of the combined phase and code observations are derived:

$$\sigma_{\Phi_{(i,j,k)}}^2 = \mu_{(i,j,k)}^2 \sigma_{\Phi}^2 \quad (10)$$

$$\sigma_{P_{(i,j,k)}}^2 = \mu_{(i,j,k)}^2 \sigma_P^2 \quad (11)$$

3. Method of triple-frequency cycle slip detection

3.1 Selection of cycle slip detection combination

The combinations of cycle slip detection should satisfy following requirements:

1) The combinations should have longer wavelengths and lower noise levels
 2) The coefficient of ionosphere should be as small as possible to reduce the influence of the ionosphere.

3) The three combinations selected must be linearly independent.

Longer wavelength can easily detect cycle slips, especially small cycle slips. If noise of combination is too loud, it will easily cause misdetection. Smaller coefficient of ionosphere can reduce the first-order time difference of ionospheric error, which will improve the success ratio of detection. Hence, we select some combinations of carrier phase in Table 1.

Table 1. Linear combination characters of triple-frequency GPS signals

(i, j, k)	$\lambda_{(i,j,k)}$	$\beta_{(i,j,k)}$	$\mu_{(i,j,k)}$
(0,0,1)	0.2550	1.7933	1
(0,1,-1)	5.8610	-1.7186	33.2415
(1,-1,0)	0.8619	-1.2833	5.7400
(4,-5,0)	1.8316	-23.2604	53.7448
(1,0,-1)	0.7514	-1.3391	4.9282
(2,0,-1)	0.1518	0.5273	1.7035
(0,1,1)	0.1247	1.7186	0.7073

3.2 EWL Combination

First, we choose code-phase combination as EWL combination. From Table 1, we can know that phase combination (0,1,-1) has longer wavelength and lower $\beta_{(i,j,k)}$ and $\mu_{(i,j,k)}$. Coefficients of code combination is (0,1,1), so EWL combination is geometry-free (GF) and ionosphere-free (IF) combination.

By differencing the ambiguities of adjacent epochs, we can obtain cycle slip of EWL combination

$$\Delta N_{EWL} = (\Delta P_{(0,1,1)} - \Delta \Phi_{(0,1,-1)}) / \lambda_{EWL} \quad (12)$$

The integer cycle slips on the EWL can be expressed as:

$$\Delta \hat{N}_{EWL} = \text{round}(\Delta N_{EWL}) \quad (13)$$

3.3 WL Combination

From Table 1, (1,-1,0) is chosen as WL combination. In the previous step, cycle slip of EWL is repaired correctly. In this step, EWL combination will be used as “pseudorange” to compute cycle slip of WL combination. The cycle slip of WL combination is determined by differencing the ambiguities at two adjacent epochs which is written as:

$$\Delta N_{WL} = [(\Delta \Phi_{EWL} - \Delta \Phi_{WL}) + (\beta_{EWL} - \beta_{WL})\Delta I + \lambda_{EWL}\Delta \hat{N}_{EWL}] / \lambda_{EWL} \quad (14)$$

Because $(\beta_{EWL} - \beta_{WL})\Delta I / \lambda_{EWL}$ is very small, so it can be ignored in the calculation process.

The integer cycle slips on the WL can be expressed as:

$$\Delta \hat{N}_{WL} = \text{round}(\Delta N_{WL}) \quad (15)$$

3.4 NL Combination

(0,0,1) is chosen as NL combination in Table 1. Similar to previous step, WL combination whose cycle slip has repaired correctly is used as the “pseudorange” to construct the GF combination. The cycle slip of third combination can be derived as:

$$\Delta N_{NL} = [(\Delta \Phi_{WL} - \Delta \Phi_{NL}) + (\beta_{WL} - \beta_{NL})\Delta I + \lambda_{WL}\Delta \hat{N}_{WL}] / \lambda_{NL} \quad (16)$$

The integer cycle slips on the NL can be expressed as

$$\Delta \hat{N}_{NL} = \text{round}(\Delta N_{NL}) \quad (17)$$

Because wavelength of NL combination is too small, so $(\beta_{WL} - \beta_{NL})\Delta I / \lambda_{NL}$ cannot be ignored.

Note that frequency f_2 and f_3 are very close, which will makes ΔI derived from φ_2 and φ_3 noisier than from the other two schemes. Hence, φ_1 and φ_3 are chosen to compute ΔI .

ΔI can be derived as:

$$\Delta I = (\Delta \lambda_1 \varphi_1 - \Delta \lambda_3 \varphi_3) / (f_1^2 / f_3^2 - 1) \quad (18)$$

3.5 Resolution of original cycle slip

The original cycle slip can be fixed correctly by the following equation:

$$\begin{bmatrix} \Delta N_1 \\ \Delta N_2 \\ \Delta N_3 \end{bmatrix} = \begin{bmatrix} 0 & 1 & -1 \\ 1 & -1 & 0 \\ 0 & 0 & 1 \end{bmatrix}^{-1} \begin{bmatrix} \Delta N_{EWL} \\ \Delta N_{WL} \\ \Delta N_{NL} \end{bmatrix} \quad (19)$$

3.6 Success rate of detection and elevation of satellite model

According to [6], the corresponding success rate can be computed as:

$$P = \Phi\left(\frac{1 + 2\delta_{\Delta N(i,j,k)}}{2\sigma_{\Delta N(i,j,k)}}\right) + \Phi\left(\frac{1 - 2\delta_{\Delta N(i,j,k)}}{2\sigma_{\Delta N(i,j,k)}}\right) - 1 \quad (20)$$

Where $\Phi(x) = \int_{-\infty}^x \frac{1}{\sqrt{2\pi}} \exp\left(-\frac{1}{2}z^2\right) dz$, $\delta_{\Delta N(i,j,k)}$ is bias of the estimated ambiguity.

According to [7], the satellite elevation-based sin function can be expressed as:

$$\sigma^2 = a^2 + b^2 / \sin^2(ele) \quad (21)$$

Where σ^2 is the variance of observations, ele is the elevation of satellite. a and b are constant values, a is determined by carrier phase measurement and b is mainly affected by the ionospheric and tropospheric delay. So a is set 2 mm and b is set 1.5 mm. The variance of EWL, WL and NL combination can be expressed as:

$$\begin{aligned} \sigma_{\Delta N_{EWL}}^2 &= 2(\mu_{P(EWL)}^2 \sigma_p^2 + \mu_{EWL}^2 \sigma_{\Phi}^2) / \lambda_{EWL} \\ &\approx 4.84 \times 10^{-4} (4 + 2.25 / \sin^2(ele)) \end{aligned} \quad (22)$$

$$\begin{aligned} \sigma_{\Delta N_{WL}}^2 &= 2(\mu_{EWL}^2 \sigma_{\Phi}^2 + \mu_{WL}^2 \sigma_{\Phi}^2) / \lambda_{WL} \\ &\approx 2.30 \times 10^{-3} (4 + 2.25 / \sin^2(ele)) \end{aligned} \quad (23)$$

$$\begin{aligned} \sigma_{\Delta N_{NL}}^2 &= 2[\mu_{WL}^2 \sigma_{\Phi}^2 + \mu_{NL}^2 \sigma_{\Phi}^2 + 4k_{13}(\beta_{NL} - \beta_{WL}) \sigma_{\Phi}^2] / \lambda_{NL} \\ &\approx 3.97 \times 10^{-3} (4 + 2.25 / \sin^2(ele)) \end{aligned} \quad (24)$$

Where $k_{13} = f_3^2 / (f_1^2 - f_3^2)$. Relationship between rate of success and elevation of GPS satellite can be presented by Figure 1.

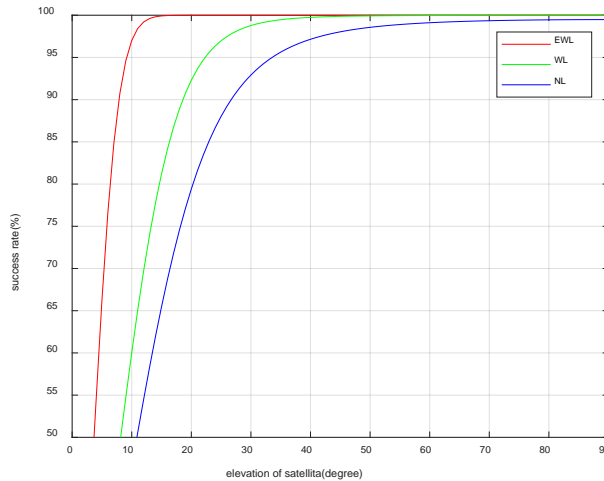


Figure 1. Success rate of EWL, WL and NL combinations.

From Figure 1, we can know that success rate of cycle slip detection is proportional to the elevation of satellite. When elevation of satellite is 20 degree, the success rates of EWL, WL and NL are 100%, 92.31% and 79.42%. When elevation is 40 degree, the success rate of EWL, WL and NL are 100%, 99.75% and 97.15%, and the overall detection success rate can reach 96.91%. Hence 40 degree can be set as threshold for triple-frequency cycle slip detection. When elevation of satellite is higher than 40 degree, the result of cycle slip detection method can ensure the reliability of the estimated cycle slips of linear combinations.

4. Experiment results and analysis

In the previous section, we analyzed the relationship between success rate of GPS triple-frequency cycle slip detection and elevation of satellite. 40 degree is set as threshold. In this section, we use triple-frequency observations of GPS—which were provided by the multi-GNSS experiment (MGEX) station JFNG on 17 July 2013—are used to verify the previous conclusions. GPS G01, G24 and G27 are tested. Figure 2 displays the time-difference ambiguities of three GPS satellites.

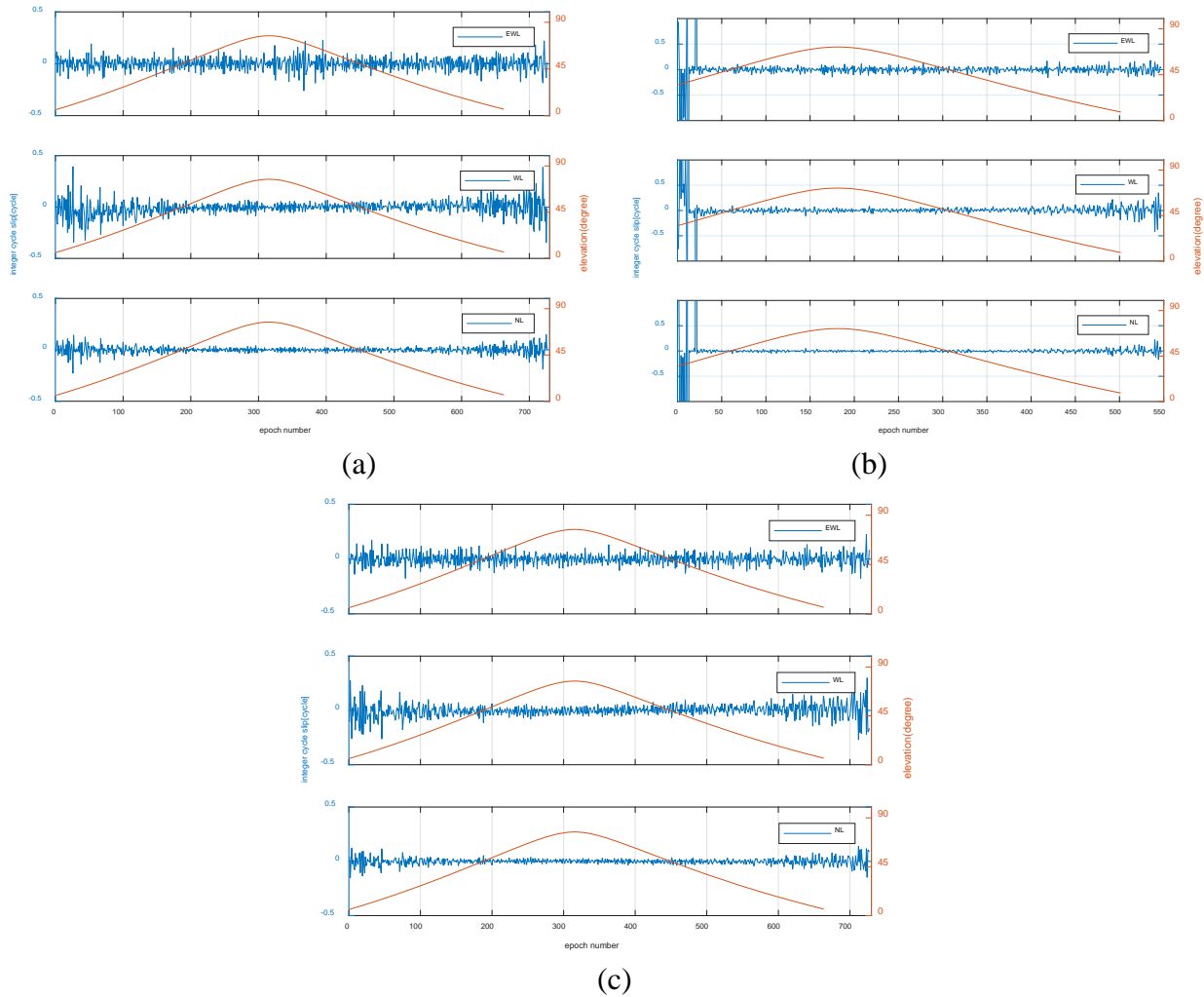


Figure 2. Cycle slips detection of triple-frequency combinations for GPS satellites (top: G01, middle: G24, bottom: G27)

From Figure 2, we can know that cycle slips detection of WL and NL combinations is inversely proportional to the elevation of satellite. Due to code observation in EWL combination, elevation has a smaller impact on EWL combination and EWL combination has bigger noise level. The detection of the cycle slip is not only affected by the elevation angle, but also the noise level of the carrier phase and pseudorange observations is also an important factor.

5. Conclusion

In this paper, we discussed the relationship between the triple-frequency cycle slip detection and elevation of satellite for GPS. According to the correlation between observation variance and the elevation of GPS satellite, the equation of detection success rate and elevation was derived. Moreover, 40 degree was set as threshold for triple-frequency cycle slip detection. In order to show the conclusions more clearly, triple-frequency data of GPS was used. The result showed that WL and NL combinations were affected by elevation of satellite and had obvious changes.

References

- [1] Zhao Q, Sun B, Dai Z, Hu Z, Shi C, Liu J (2015) Real-time detection and repair of cycle slips in triple-frequency GNSS measurements. *GPS Solutions* 19 (3): 381–391
- [2] Huang L, Lu Z, Zhai G, Ouyang Y, Huang M, Lu X, Wu T, Li K (2016) A new triple-frequency cycle slip detecting algorithm validated with BDS data. *GPS Solutions* 20 (4): 761–769
- [3] Yao Y, Gao J, Wang J, Hu H, Li Z (2016) Real-time cycle-slip detection and repair for Bei Dou triple-frequency undifferenced observations. *Empire Survey Review* 48 (350)
- [4] Li B, Qin Y, Li Z, Lou L (2016) Undifferenced cycle slip estimation of triple-frequency Bei Dou signals with ionosphere prediction. *Marine Geodesy* 39 (5): 348–365
- [5] Feng Y (2008) GNSS three carrier ambiguity resolution using ionosphere-reduced virtual signals. *Journal of Geodesy* 82 (12): 847-862
- [6] Teunissen PJG (2001) Integer estimation in the presence of biases. *Journal of Geodesy* 75 (7-8): 399-407
- [7] Jin S, Wang J, Park PH (2005) an improvement of GPS height estimations: stochastic modeling. *Earth Planets Space* 57: 253–259